BEDROCK DELINEATION BY A SEISMIC REFLECTION AND REFRACTION SURVEY AT TOOELE ARMY DEPOT, UTAH

David Sheley and Jianhua Yu

March 13, 2001

SUMMARY

A seismic reflection/refraction survey was conducted at Tooele Army Depot (TEAD), Utah to determine the depth to bedrock. Two independent processing flows were performed. The first used standard seismic reflection processing to generate a seismic reflectivity image of the subsurface, and the second used first-arrival traveltimes to generate a velocity model of the subsurface. Reflection processing steps included trace editing, deconvolution, bandpass filtering, velocity analysis, NMO correction, residual statics, stacking, and F-X prediction filtering. It was found that iterative velocity analysis, NMO and, residual static analysis significantly improves focusing of reflection energy. The seismic reflectivity section clearly shows a large amplitude reflector that correlates well with the expected depth of the bedrock at two of the three wells along the profile. At the location of the third well there is a strong correlation of the shape of the seismic bedrock reflector with the actual bedrock outcrop in the northern part of the line. However, the seismic bedrock reflector is not continued all the way to the surface in the seismic section because of the limited acquisition geometry. The seismic bedrock interface is mostly continuous all along the seismic profile and is at the estimated depth of the bedrock interface. The general features of the velocity tomogram supports the above interpretation, except the tomogram has a much lower spatial resolution. Although our seismic images appear to be adequate for identification of bedrock geometry, a more reliable seismic section could be obtained with a seismic survey with a more dense shot and receiver spacing.

SURVEY OBJECTIVE AND LOCATION

The objective of this survey was to determine the depth to the subsurface bedrock interface along a 2.64 km (1.64 mi) transect in the Tooele Army Base using seismic reflection and refraction imaging. Depth to bedrock, as constrained by well information, varies from about 3 m (about 19 ft) to deeper than 90 m (about 300 ft).

The survey location, shown as the northwest to southeast trending red line in Figure 1, was conducted at the northeastern corner of TEAD and roughly parallels

state highway 112. The depth to bedrock in well B-9 is roughly 3 m (about 20 ft), in well C-14 it is greater than 90 m (about 300 ft) and in C-30 bedrock it is 297 ft (about 91 m). For the purposes of this paper the northwest end of the acquisition line is 0 m and the southwest end is 2640 m. All of the profiles shown in this paper have the northwest end at the right and the southeast at the left.

ACQUISITION EQUIPMENT AND SURVEY GEOMETRY

Data was recorded with a 120 channel Bison seismograph and 120 40-Hz vertical-component geophones placed at five-meter (16.4 ft) intervals. A 500-pound elastic weight drop (EWG) source was activated at 2.5-meter intervals for a total of 1056 common shot gathers. The source is trailer mounted and a gasoline hydraulic pump raises the source. Each shot gather was recorded for 1.5 seconds at a sampling rate of 0.001 seconds for a total of 1500 samples per trace, with 120 traces per shot gather. A split spread technique was utilized, maintaining at least forty-eight traces (240 m) on either side of the source.

DATA ANALYSIS

The data were analyzed by two independent techniques: Reflection processing to produce a stacked section, and first-arrival refraction tomography to produce a velocity tomogram.

Reflection Processing and Results

A standard processing flow for shallow reflection data was followed (Figure 2). Following acquisition, the data were checked and two shot gathers were deleted for stacking problems. After resorting to the common receiver gather (CRG) domain the data were checked again and several ($\sim$ 20) CRG's were muted entirely or partially due to bad geophones. Ormsby bandpass filtering from 15 to 50 Hz with a 10 Hz ramp on either side was then applied followed by automatic gain control (AGC) with a 500 ms window. To increase the signal to noise ratio we then muted the coherent noise arrivals of the refracted and surface waves similar to Baker *et. al.* (1998). Since small errors in normal moveout (NMO) velocity estimates may lead to defocusing of the reflection energy during stacking, three iterations of velocity analysis, NMO correction, and residual statics were performed to ensure the correct stacking velocity. After stacking the common midpoint (CMP) gathers, the data were post-processed to enhance the coherent reflectors. This included bandpass filtering, amplitude scaling, F-X prediction filtering, weighted trace mixing, and AGC scaling. It was determined that iterative velocity analysis, NMO and, residual static analysis were key processing steps in getting a final section with coherent reflectors.

The final stacked and post-processed image can be seen as Figure 3 in time on the right and after time to depth conversion using velocities from the tomography result on the left. Note the large amplitude reflector that is nearly continuous all along the

profile. Near the outcrop, the reflector geometry becomes steeply dipping but does not approach the surface commensurate with the actual outcrop. This is because the acquisition geometry and processing were not tuned to such steep events. It is expected that further processing and a tighter receiver geometry would have given the expected outcrop image at the surface.

In order to locate any strong diffractors depth migration was applied. A 20 degree aperture was used to limit strong artifacts. The result, given in Figure 4, shows strong correlation to the time to depth converted stacked section.

To partly validate the seismic image, several processed CMP gathers are displayed in Figures 5 and 6. Note that in some of the CMP gathers the reflection from the bedrock interface is obvious while in others it is not as clear.

Refraction Tomography Processing and Results

Approximately 117,000 first arrival traveltimes were picked from the data. A single shot gather with picked first arrival traveltimes is given as Figure 7. These picks were inverted using a 2-D refraction tomographic method (Nemeth *et. al.*, 1997; Morey and Schuster, 1999). This procedure produced the velocity image in Figure 8 and the associated raypath density diagram in Figure 9. The graph of residual versus iteration number is depicted in Figure 10, and shows convergence at a RMS residual of 7 ms. This is the expected noise level for the tomograms because the frequency content of the signal was estimated to be no more than 100 Hz. Areas of the raypath density diagram with large numbers of rays correspond to good coverage and can be considered most reliable. Conversely, less dense areas of the diagram have less ray coverage and are less reliable.

DISCUSSION AND CONCLUSION

A seismic reflection/refraction survey was conducted at Tooele Army Depot (TEAD), Utah to determine the depth to bedrock. Reflection processing steps included trace editing, deconvolution, bandpass filtering, velocity analysis, NMO correction, residual statics, stacking, and F-X prediction filtering. It was found that iterative velocity analysis, NMO and, residual static analysis significantly improves focusing of reflection energy, without which there was almost no believable reflection signal from the bedrock. The seismic reflectivity section clearly shows a large amplitude reflector that correlates well with the expected depth of the bedrock at two of the three wells.

At the location of the third well there is a strong correlation of the shape of the seismic bedrock reflector with the actual bedrock outcrop in the northern part of the line. However, the seismic bedrock reflector is not continued all the way to the surface in the seismic section because of the limited acquisition geometry. The seismic bedrock interface is mostly continuous all along the seismic profile and is at the estimated depth of the bedrock interface. The general features of the velocity tomogram supports the above interpretation, except the tomogram has a much lower spatial resolution. Although our seismic images appear to be adequate for identification of

bedrock geometry, a more reliable seismic section could be obtained with a seismic survey with half the shot and receiver spacing.

A comparison of the different results (velocity tomography, stacked reflection section, and depth migrated section) is given as Figure 11. Note that there is a 4X vertical exaggeration in each of the images. The tomogram in this image has a curtailed colormap, i.e., only the velocities between 500 m/s and 3000 m/s are used to generate the colormap. Figure 12 adds well information to Figure 11. Stars indicate the location that the wells intersected bedrock. The circle denotes the depth at which well C-14 was halted without encountering bedrock. The bedrock contact is interpreted in Figure 13. The seismic results and well information were used to constrain the bedrock location. We believe that there is a high confidence level for the delineation of the bedrock boundary in many parts of the seismic section. This confidence level is obtained by examining many CMP gathers for obvious reflections, for example Figures 5 and 6. Furthermore, the velocity tomogram gives low-frequency validation to the reflectivity section.

REFERENCES

Baker, G., Steeples, D., and Drake, D., 1998, Muting the noise cone in near-surface reflection data: An example from southeastern Kansas, *Geophysics*, **63**, 1332-1338.

Nemeth, T., Normark, E., and Qin, F., 1997, Dynamic smoothing in cross-well traveltime tomography, *Geophysics*, **62**, 168-176.

Morey, D., and Schuster, G.T., 1999, Paleoseismicity of the Oquirrh fault, Utah from shallow seismic tomography, *Geophys. J. Int.*, **138**, 25-35.

Yilmaz, O., 1987, *Investigations in Geophysics no. 2: Seismic Data Processing*, Society of Exploration Geophysicists, Tulsa, OK.

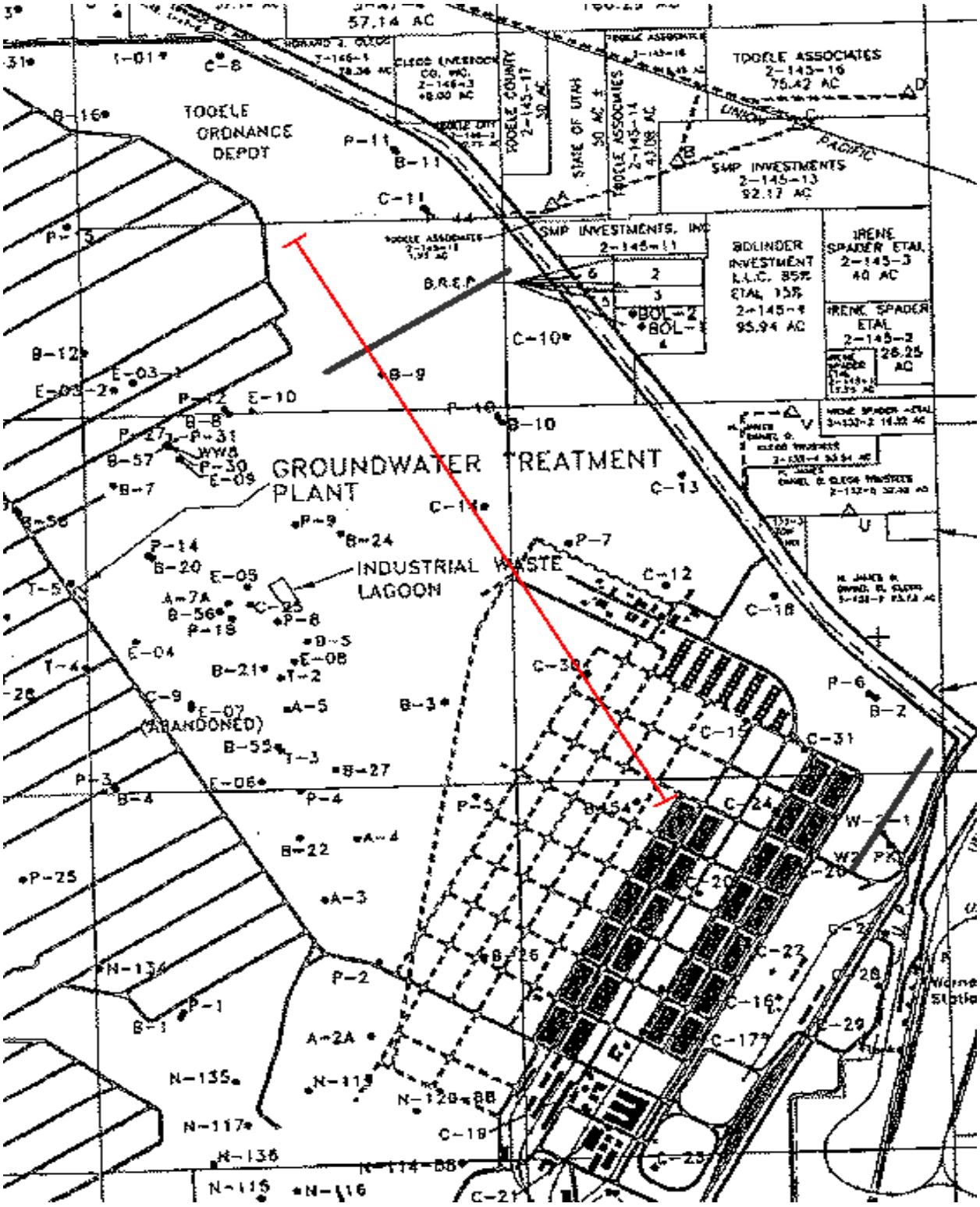

Figure 1: Location of seismic refraction/reflection line. The total line length is 2640 m (1.64 mi.). Sources were placed every 2.5 m. and receivers every 5 m. North is at the top of the map.

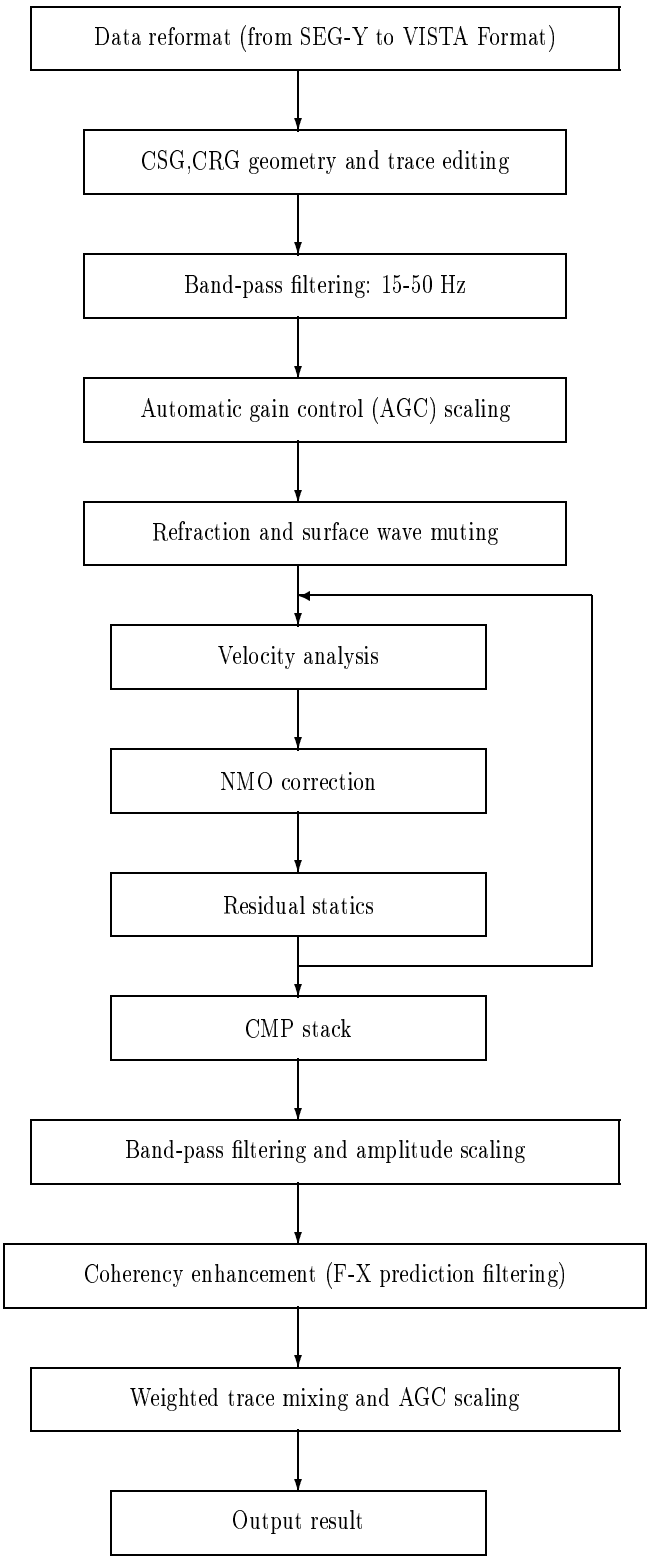

Figure 2: Seismic reflection processing flow.

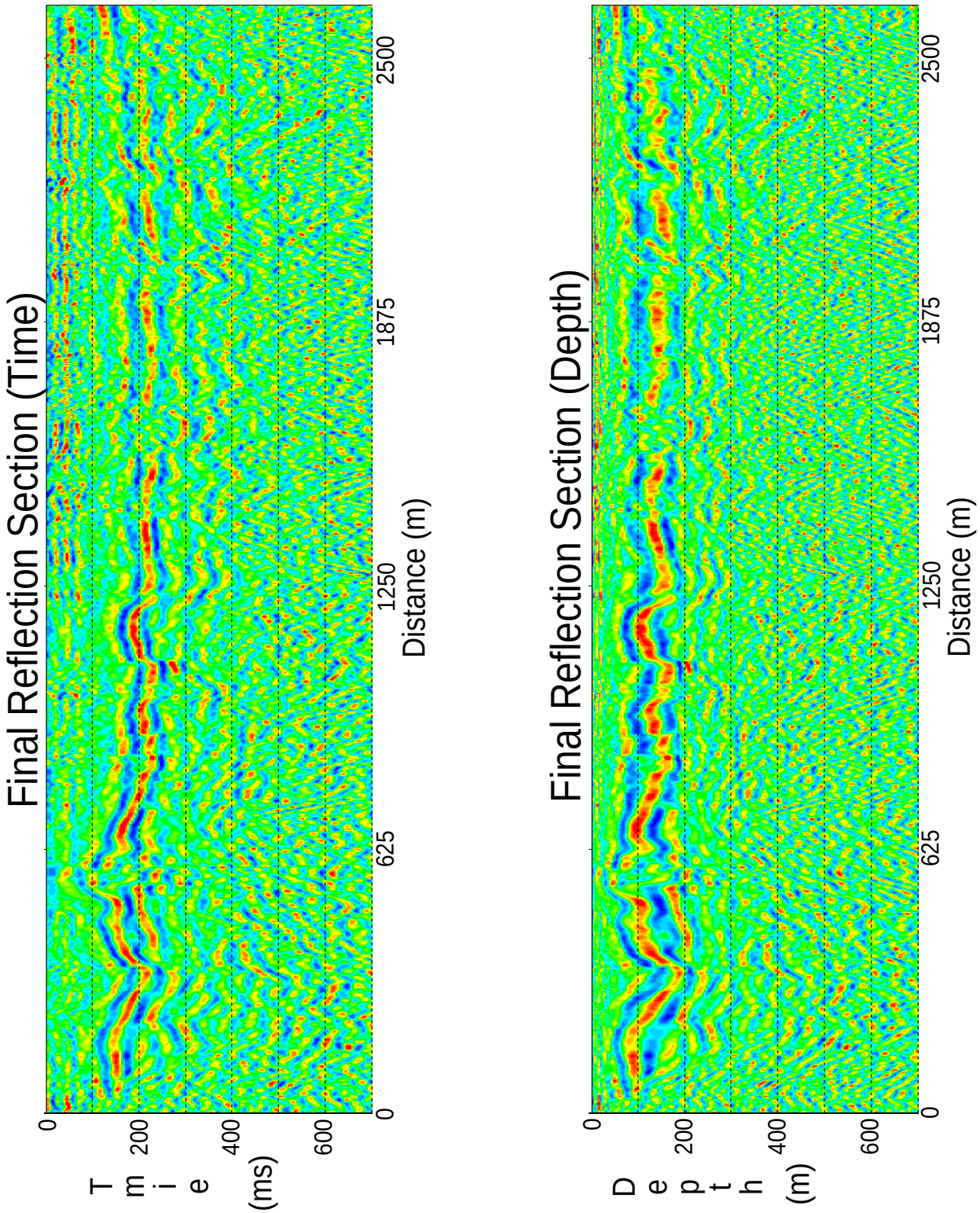

Figure 3: Final stacked reflection section in time (right) and depth (left). The abscissa is offset in meters and the ordinate is time in milliseconds for the time plot and depth in meters for the depth plot.

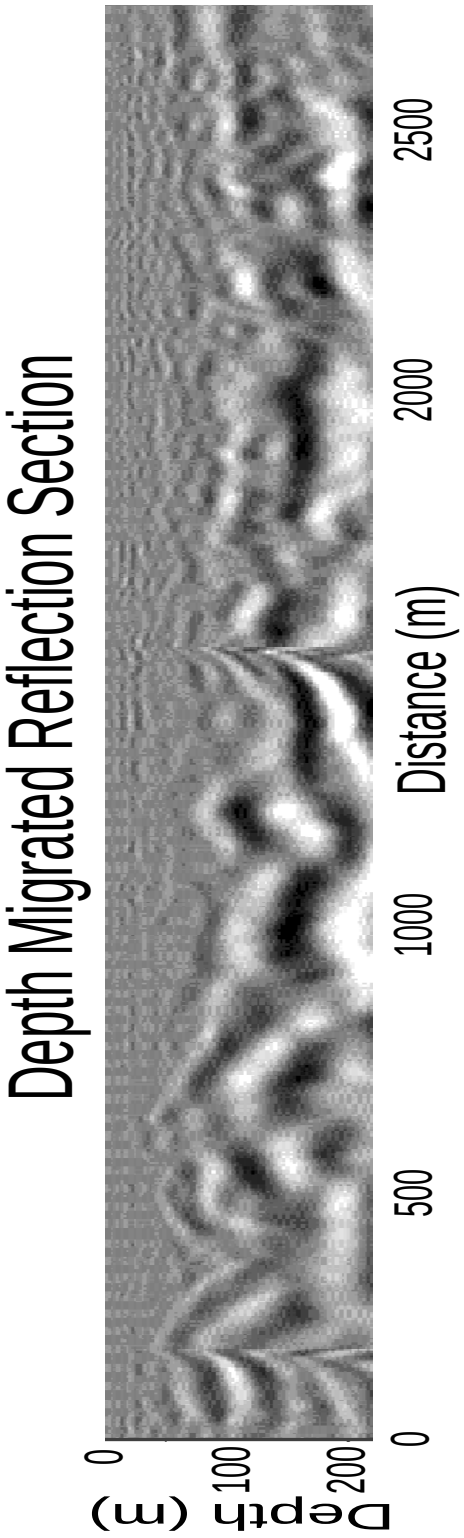

Figure 4: Depth migrated image using the tomographic velocity model (Figure 8).

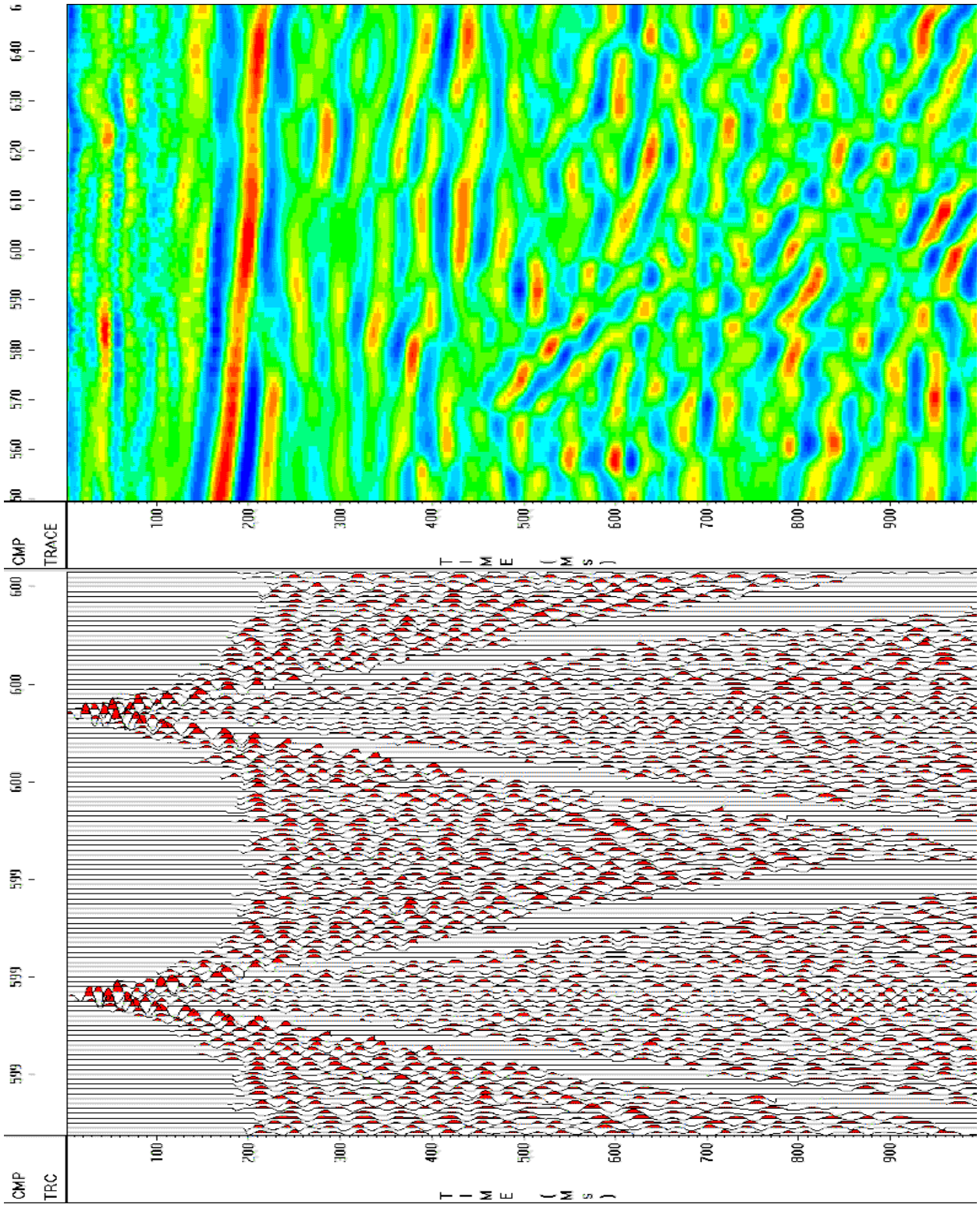

Figure 5: CMP 600

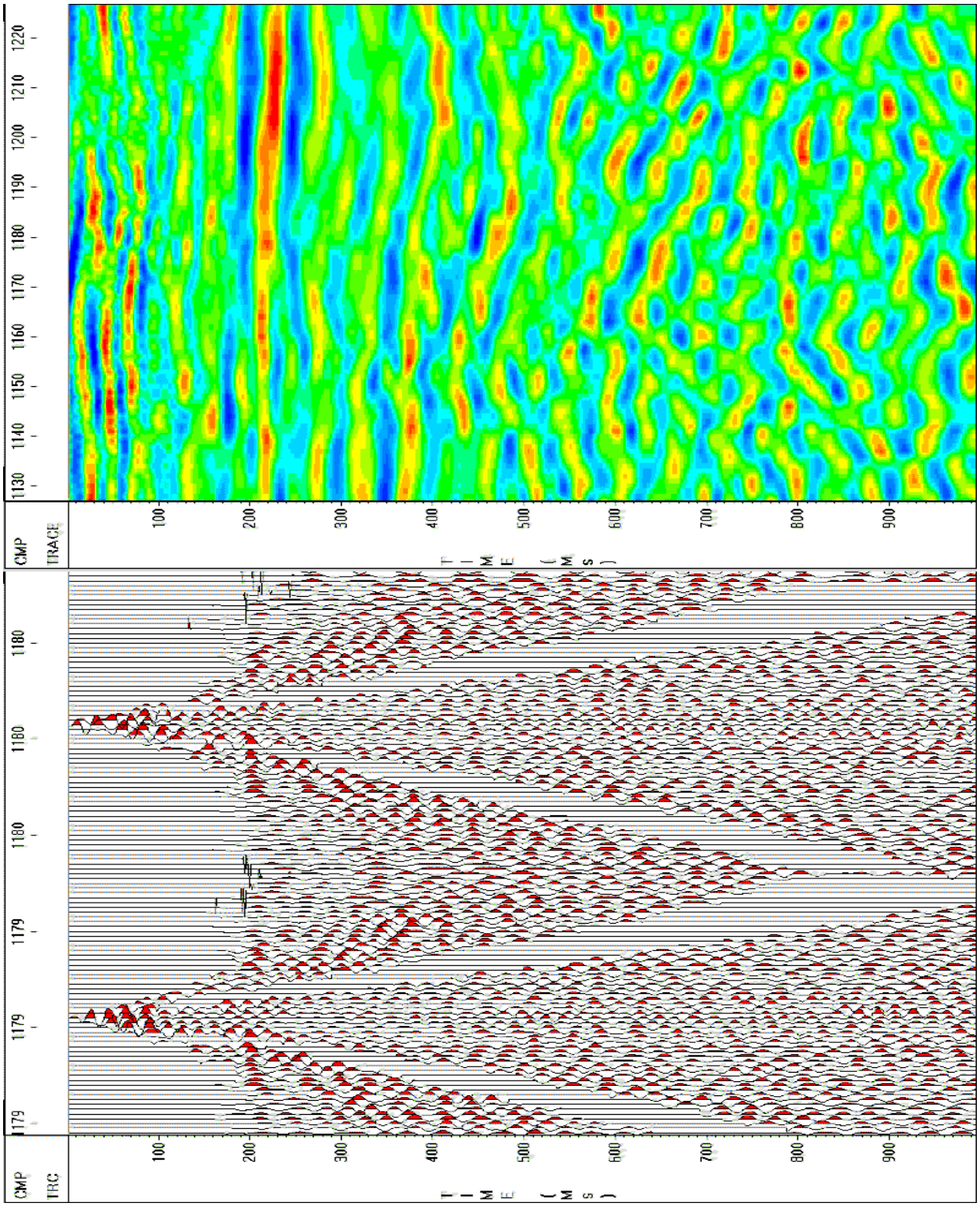

Figure 6: CMP 1180

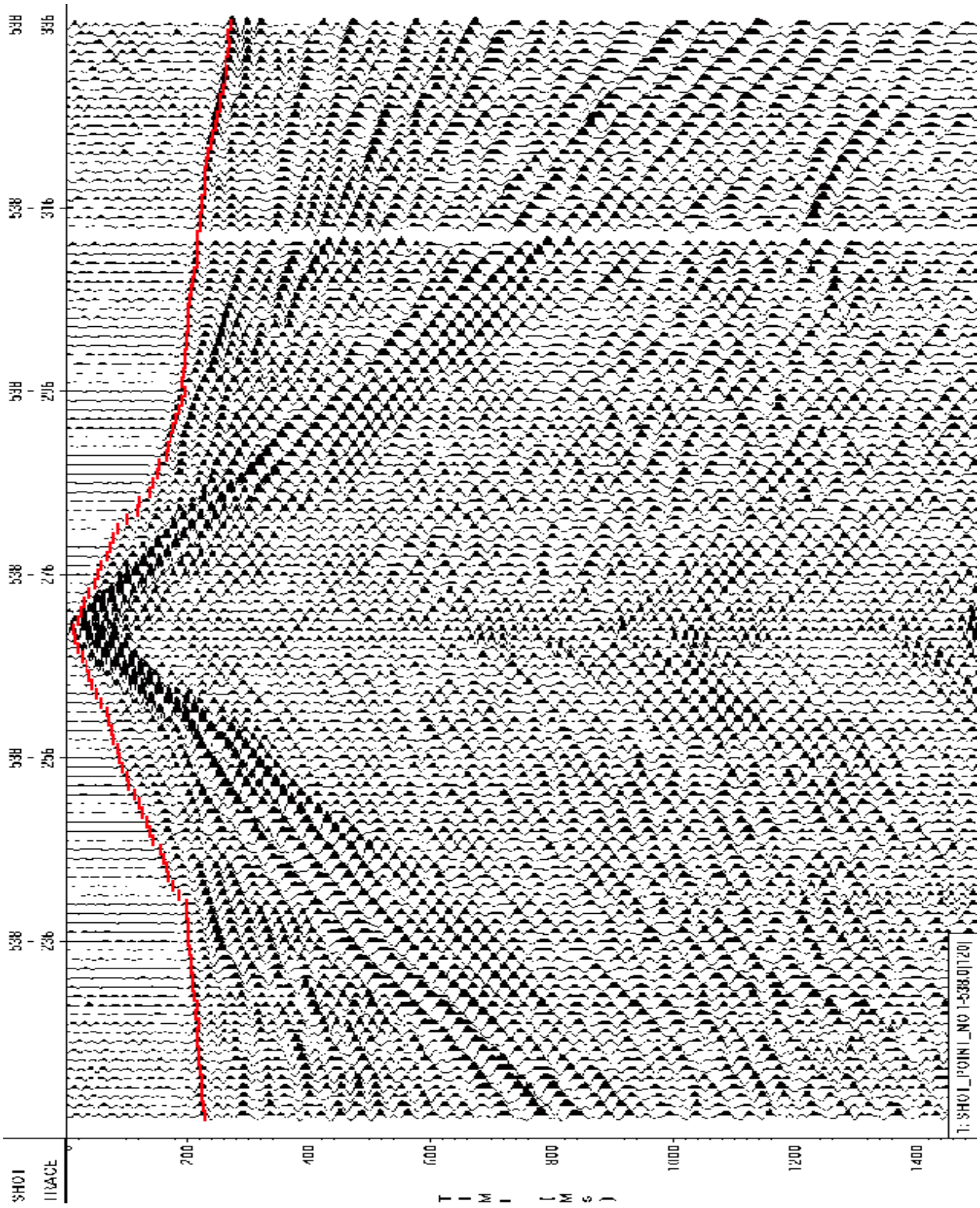

Figure 7: First arrival refraction picks for shot number 538.

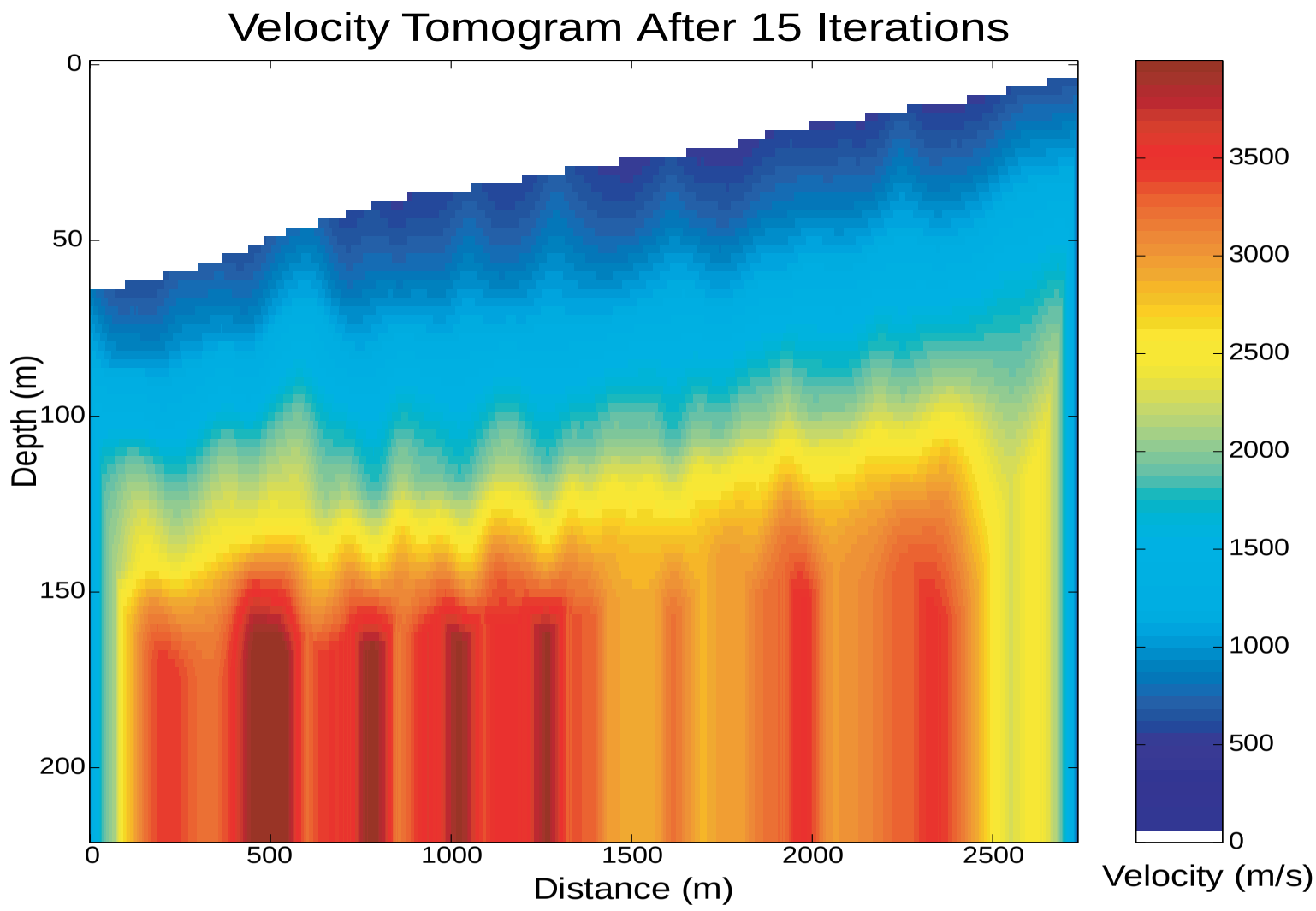
Velocity Tomogram After 15 Iterations
Depth (m)
0
50
100
150
200
0
500
1000
1500
2000
2500
Distance (m)
3500
3000
2500
2000
1500
1000
500
0
Velocity (m/s)

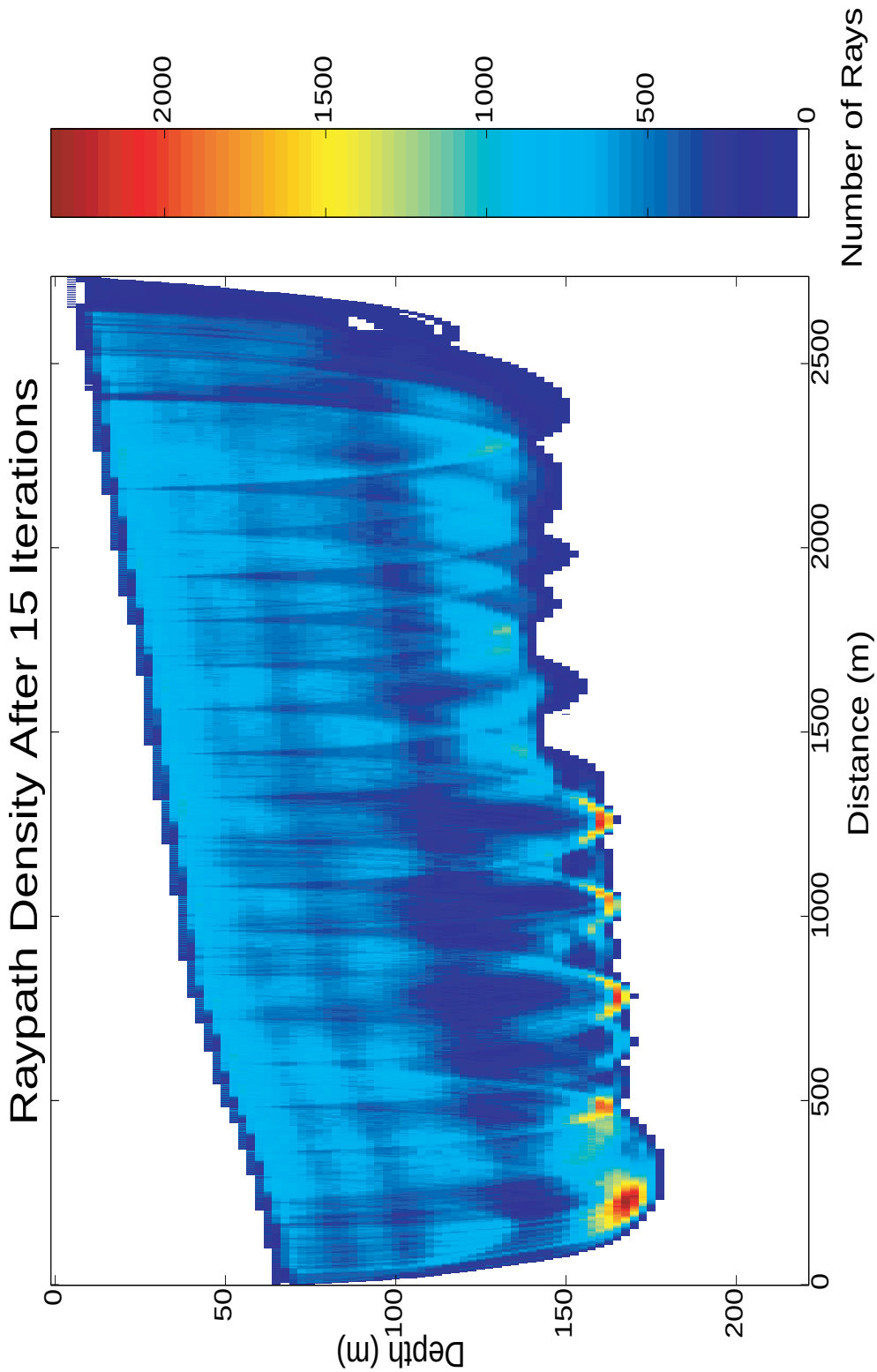

Figure 9: Raypath Density Diagram.

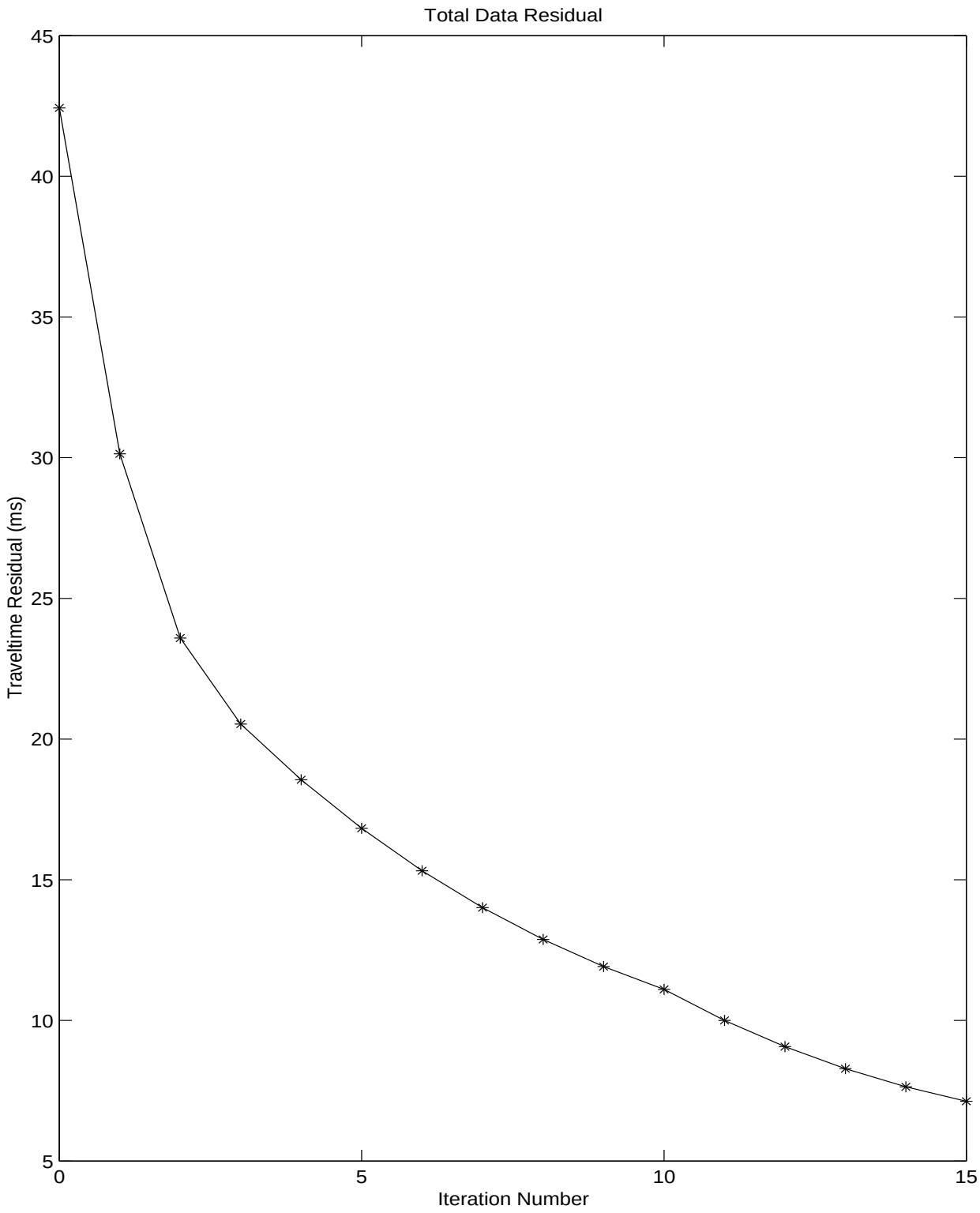

Figure 10: Data Residual vs Iteration number.

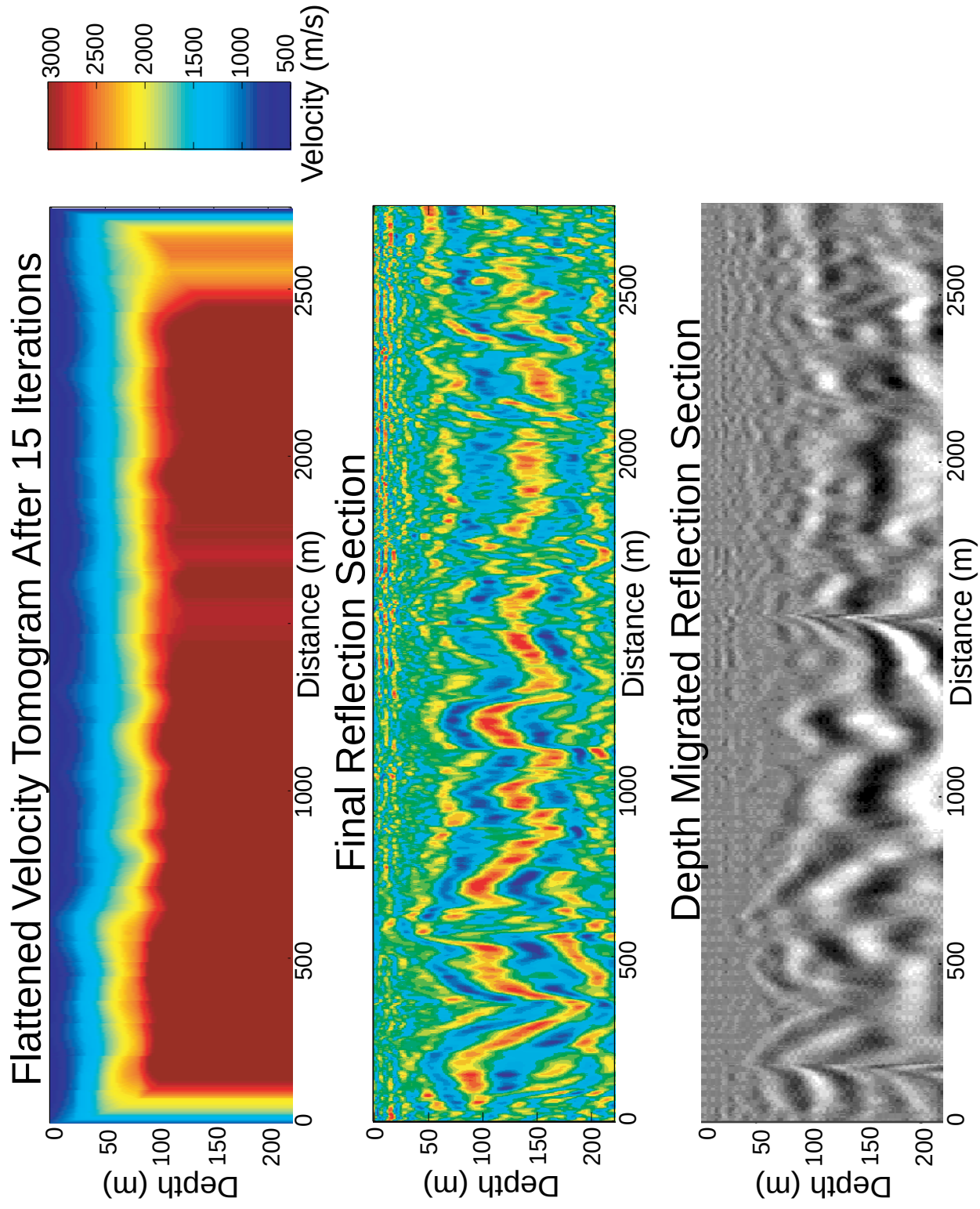

Figure 11: Comparison of velocity tomogram, final stacked section (in depth), and depth migrated reflection section.

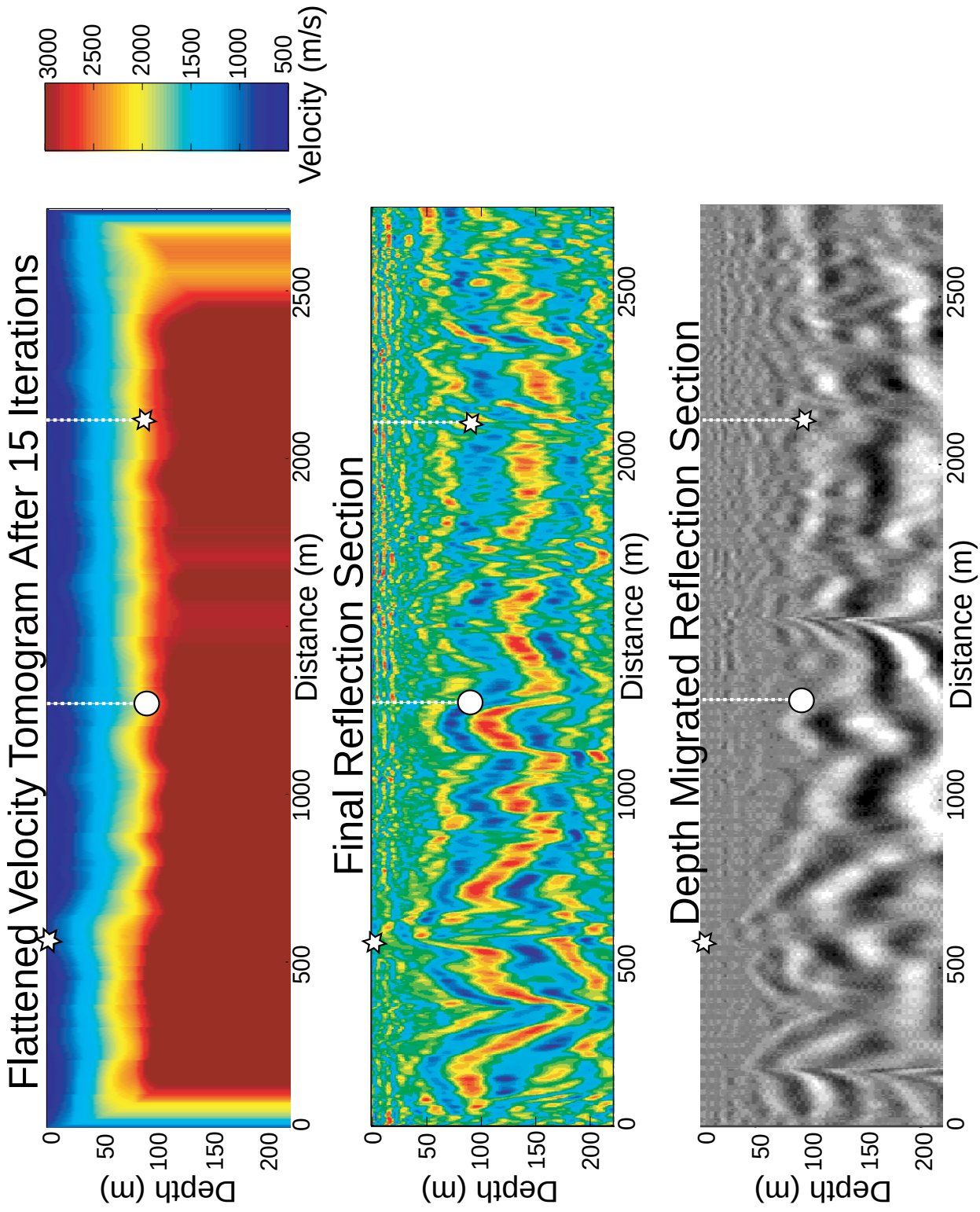

Figure 12: Comparison of velocity tomogram, final stacked section (in depth), and depth migrated reflection section. Well locations are denoted with symbols. Stars indicate locations where wells intersected bedrock. The circles denote the location and depth of well C-14 which did not encounter bedrock.

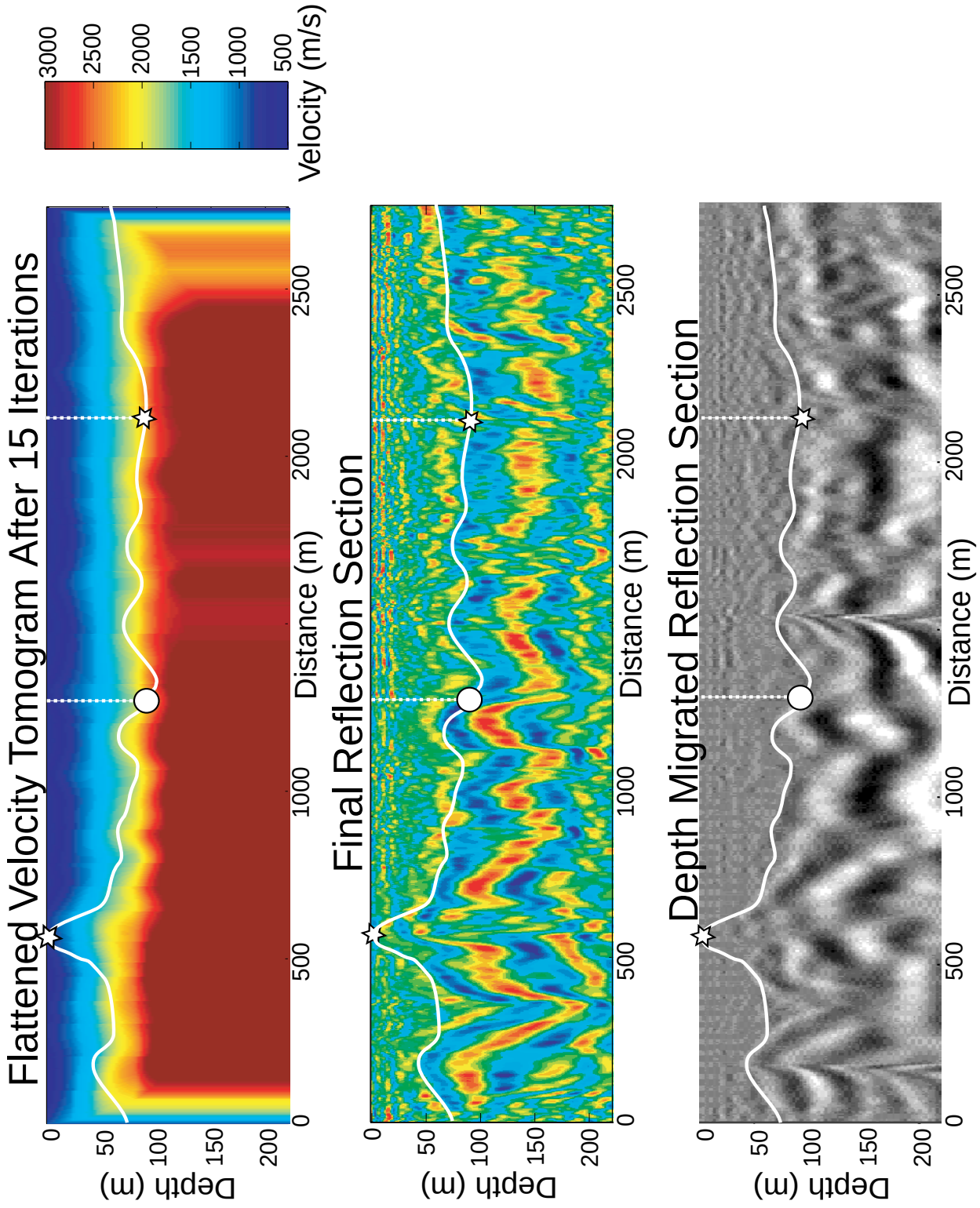

Figure 13: Similar to Figures 11 and 12 with an interpretation drawn as the sinuous white line. All three images and well information were synthesized to generate the interpretation.